rearrangement in which C4 of a pentose is excised and C3 and C5 are reconnected intramolecularly. The data offer no information concerning whether the more proximal precursor is a pentose or a pentulose, nor is it possible to draw conclusions about which pentose/pentulose stereoisomer (e.g., ribose, xylose, etc.) is employed in this intriguing biosynthesis. Labeling experiments in vitro are under way to investigate the nature of intermediates in this pathway.

Acknowledgment. We thank Dr. H. Otsuka, now at Hiroshima University, Japan, for the preparation of [2,3-$^{13}C_2$]succinate and Angelika Kohnle and Kay Kampsen for secretarial assistance. We also thank Dr. David H. Bown for helpful discussions. Financial support is acknowledged from the Deutsche Forschungsgemeinschaft and the Fonds der Chemischen Industrie (grants to A.B.), the National Institutes of Health (grant to P.J.K. and H.G.F.), and the Alexander von Humboldt Foundation (fellowship to P.J.K. and Senior US Scientist Award to H.G.F.).

Registry No. *o*-MeC_6H_4Me, 95-47-6; riboflavin, 83-88-5; acetate, 64-19-7; ribose, 50-69-1; glycerol, 56-81-5; glucose, 50-99-7; succinate, 110-15-6.

Gold Carbonyl, Au(CO): Matrix Isolation ESR Study

Paul H. Kasai* and Paul M. Jones

Contribution from IBM Instruments, Inc., Orchard Park, Danbury, Connecticut 06810.
Received April 12, 1985

Abstract: ESR spectra of gold(0) monocarbonyl generated in argon matrices by cocondensation of gold atoms and CO molecules were observed and analyzed. The **g** tensor and the ^{197}Au and ^{13}C hyperfine-coupling tensors of the complex were determined. Also seen in the spectra were effects of the Au nuclear quadrupole moment; the effects were demonstrated, and the nuclear quadrupole coupling tensor was determined. It is shown that the complex is formed by the dative interaction of the lone-pair electrons of CO with a vacant sp_σ orbital of the metal atom and the back-donation from the metal d_π orbitals into the antibonding π^* orbitals of CO. The unpaired electron is in the sp_σ orbital of the metal atom pointing away from the ligand.

It has been shown that otherwise unstable carbonyls of group 11 metal atoms could be generated by cocondensation of the metal atoms and CO molecules in rare gas matrices at cryogenic temperature (4–20 K).[1-4] The thorough analyses of the vibrational spectra of the resulting matrices by Ozin et al. clearly established the formation of $Cu(CO)_n$ (n = 1, 2, 3),[2] $Ag(CO)_n$ (n = 1, 2, 3),[3] and $Au(CO)_n$ (n = 1, 2)[4] in the respective systems. They also showed that the mono- and dicarbonyl species were linear, while the tricarbonyls were trigonal planar.

Recently we have reported on the ESR (electron spin resonance) spectra of Cu(CO) and $Cu(CO)_3$ and of Ag(CO) and $Ag(CO)_3$ generated in argon matrices.[5,6] The ESR spectra showed that the semifilled orbital of Cu(CO) is an sp_σ hybrid orbital of the Cu atom pointing away from the ligand, while the semifilled orbitals of $Cu(CO)_3$ and $Ag(CO)_3$ represent the back-donation from the valence p_π orbital of the metal atom into the antibonding π^* orbitals of the CO moiety. In contrast, the ESR spectrum of Ag(CO) was essentially that of slightly perturbed Ag atoms; the magnitude of the observed ^{13}C hf (hyperfine) interaction was that expected from a CO molecule separated by the nearest neighbor distance of the host lattice. The dicarbonyls of these atoms with a linear structure would have a $^2\Pi$ ground state; their ESR spectra would hence be broadened beyond detection.

Reported below is an account of the ESR spectra observed when the Au atoms and CO molecules were cocondensed in argon matrices. Unlike the situations encountered in the Cu and Ag cases, only the signals of the monocarbonyl, Au(CO), were observed in addition to those of isolated metal atoms. The result is consistent with the conclusion reached earlier that $Au(CO)_3$ is not formed.[4] The spectral analysis revealed that Au(CO) is a bona fide complex with a bonding scheme similar to that of Cu(CO). The semifilled orbital is hence the sp_σ hybrid orbital of the Au atom pointing away from CO. The observed spectra also showed effects of the Au nuclear quadrupole interaction; the effects were demonstrated and the Au nuclear quadrupole coupling tensor was determined.

Table I. Observed and Computed Resonance Positions of Au(CO) in Argon Matrix[a]

	hyperfine component (m_I)			
signals	+3/2	+1/2	−1/2	−3/2
$H_\parallel$ (obsd)	2369	2889	3520	4271
$H_\parallel$ (com)	2369	2888	3521	4271
$H_\perp$ (obsd)	2478	2991	3637	4395
$H_\perp$ (com)	2478	2990	3636	4395

[a] Given in G, accuracy ±1 G, and microwave frequency = 9.425 GHz.

Experimental Section

A liquid helium cryostat system that would enable trapping of vaporized metal atoms in an inert gas matrix and examination of the resulting matrix by ESR has been described earlier.[7a] In the present series of experiments, gold atoms were generated from a resistively heated (~1500 °C) tantalum cell and were trapped in rare gas matrices containing controlled amounts of carbon monoxide (1–30%). Because of the wetting and alloying properties of molten gold, gold pellets were first placed in an alumina tube, capped with a molybdenum plug, and then placed in the tantalum cell. The gold atoms effused through an opening drilled through the Ta and alumina walls. From the line width of the ESR signals of the Au atoms, the Au atom concentration was estimated to be ~0.1%.[7b]

The ESR spectrometer used was an IBM Model ER200D. A low frequency field modulation (375 Hz) was used for the signal detection. All the spectra were obtained while the matrix was maintained at ~4 K. The spectrometer frequency locked to the sample cavity was 9.426 GHz, and the microwave power typically employed was ~20 μW. For photoirradiation of the matrix, a high-pressure xenon-arc lamp (Oriel, 1 kW unit) was used with a set of sharp cutoff filters.

(1) Ogden, J. S. *J. Chem. Soc., Chem. Commun.* **1971**, 978.
(2) Huber, H.; Künding, E. P.; Moskovits, K.; Ozin, G. A. *J. Am. Chem. Soc.* **1975**, *97*, 2097.
(3) McIntosh, D.; Ozin, G. A. *J. Am. Chem. Soc.* **1976**, *98*, 3167.
(4) McIntosh, D.; Ozin, G. A. *Inorg. Chem.* **1977**, *16*, 51.
(5) Kasai, P. H.; Jones, P. M. *J. Am. Chem. Soc.* **1985**, *107*, 813.
(6) Kasai, P. H.; Jones, P. M. *J. Phys. Chem.* **1985**, *89*, 1147.
(7) (a) Kasai, P. H. *Acc. Chem. Res.* **1971**, *4*, 329. (b) Kittel, C.; Abraham, E. *Phys. Rev.* **1953**, *90*, 238.

0002-7863/85/1507-6385$01.50/0

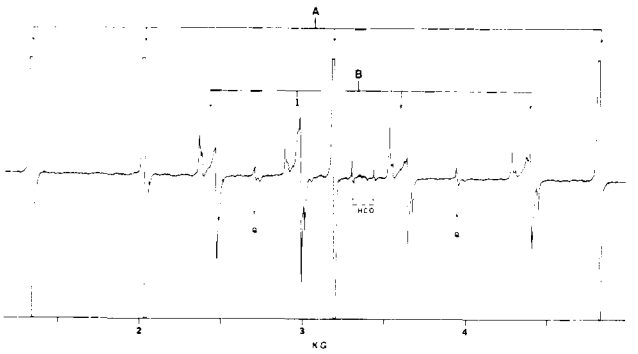

Figure 1. ESR spectrum observed from the Au/CO(2%)/Ar system. The signals labeled A are due to isolated Au atoms and those labeled B are due to Au(CO). The signals labeled Q are due to forbidden transitions caused by the quadrupole effect. See text.

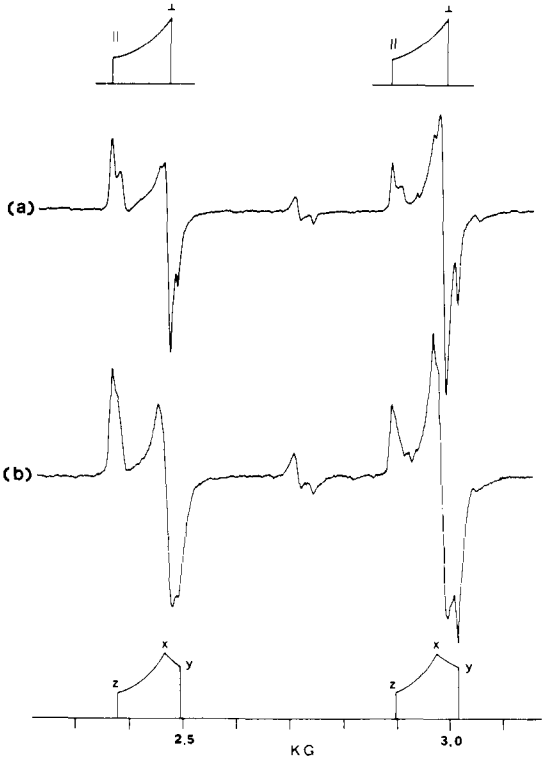

Figure 2. The lower field components (m_I = +3/2 and +1/2) of the B signals observed from (a) the Au/CO(2%)/Ar system and (b) the Au/CO(4%)/Ar system. The absorption patterns of the recognized axially symmetric and orthorhombic systems are indicated.

Research grade argon and CP grade carbon monoxide were obtained from Matheson, and ^{13}C-labeled (enrichment >99%) carbon monoxide was obtained from MSD Isotopes.

Results

The ground-state electronic configuration of Au atom is $5d^{10}6s^1$. The ESR spectrum of Au atoms isolated in rare gas matrices has been reported earlier.[8] The spectrum comprises a sharp, widely spaced quartet due to the hf interaction with the ^{197}Au nucleus (natural abundance = 100%, $I = {}^3/_2$, and $\mu = 0.1439\beta_n$).

Figure 1 shows the ESR spectrum observed from the Au/CO(2%)/Ar system. The sharp quartet indicated by letter A is that due to isolated Au atoms. The signals of present interest are those indicated by letter B. As shown in the figure, they too constitute a quartet, though with significantly reduced spacings and with additional complexity due to the anisotropies of the **g** tensor and the ^{197}Au hyperfine coupling tensor. Other signals seen in the figure are two signals indicated by letter Q situated approximately midway between the outer pairs of quartet B and a weak doublet due to inadvertently formed formyl radicals, HCO.[9]

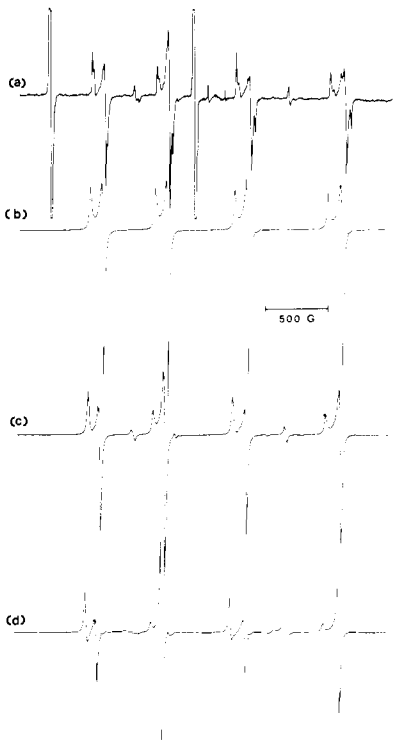

Figure 3. ESR spectra of Au(CO): (a) observed from the Au/CO(2%)/Ar system, (b–d) simulated based on the **g** tensor and the ^{197}Au hyperfine-coupling tensor given in the text and assumed value of $P_\parallel$ = 0, 45, and 75 G, respectively.

As the concentration of CO in the Au/CO/Ar system was varied from 1 to 30%, we noted that (1) the A signals decreased gradually and were not observed at all when [CO] = 30%, (2) the B signals grew initially with increasing CO concnetration, reached the optimum intensity at [CO] = 15%, and were not observed when [CO] = 30%, and (3) the color of the matrix changed from pink at [CO] = 1%, to purple at [CO] = 10%, and to dark intense purple at [CO] = 30%.

On the basis of the observations listed above and in cognizance of the results obtained in the IR study by Ozin et al.,[4] we concluded that (1) the B signals are due to the monocarbonyl, Au(CO), (2) the purple color of the matrix is due to the $^2\Pi_u \rightarrow {}^2\Pi_g$ transition of the dicarbonyl, $Au(CO)_2$, at 520 nm as assigned by Ozin et al.,[4] and (3) the tricarbonyl, $Au(CO)_3$, is not formed.

Figure 2a shows, in an expanded scale, the lower field components of the B quartet observed from the Au/CO(2%)/Ar system. It is evident that each component is a superposition of the powder pattern expected from an axially symmetric system and that expected from an orthorhombic system.[10] Figure 2b shows the spectrum (the same region) observed from the Au/CO(4%)/Ar system. That the relative intensity of the orthorhombic system increases with increasing CO concentration is clearly shown. The axially symmetric pattern is hence attributed to Au(CO) isolated in the host lattice and the orthorhombic pattern to Au(CO) perturbed by the presence of the second CO in the nearest neighbor sphere. The position of the second CO must be such that conversion to dicarbonyl $Au(CO)_2$ is not easily achieved at ~4 K. Irradiation of the matrix with "yellow light" (a xenon arc lamp with a filter for sharp cutoff at 500 nm) did not alter the relative intensities of the two components. Hereinafter we shall limit our discussion to the spectra of "isolated" Au(CO).

The observed resonance positions of the B signals (of axial symmetry) are given in Table I. The four Au hyperfine com-

(8) Kasai, P. H.; McLeod, D., Jr. *J. Chem. Phys.* **1971**, *55*, 1566.
(9) Adrian, F. J.; Cochran, E. L.; Bowers, V. A. *J. Chem. Phys.* **1962**, *36*, 1661.
(10) For analyses of ESR powder patterns, see, for example: Ayscough, P. B. "Electron Spin Resonances in Chemistry"; Methuen: London, 1967; pp 323–332.

Table II. The **g** Tensors and the Hyperfine Coupling Tensors of Cu(CO), Ag(CO), and Au(CO) and the Quadrupole Coupling Tensor ($P_\parallel$) of Au(CO) (Coupling Tensors Given in MHz)[a]

			metal nucleus		^{13}C		
carbonyl	$g_\parallel$	$g_\perp$	$A_\parallel$	$A_\perp$	$A_\parallel$	$A_\perp$	ref
Cu(CO)	1.998 (1)	1.995 (1)	4174 (2)	4126 (2)	173 (6)	184 (6)	5[b]
Ag(CO)	1.9998 (6)	2.0003 (6)	1778 (1)	1792 (1)	42 (3)	36 (3)	6
Au(CO)	1.9791 (6)	1.9105 (6)	1742 (1)	1686 (1)	316 (6)	332 (6)	this work
			$P_\parallel$ = 125 (14)				

[a] The hyperfine and the quadrupole coupling tensors of the metal nuclei are for ^{63}Cu, ^{107}Ag, and ^{197}Au in the respective complexes. [b] The ^{13}C hyperfine tensor of Cu(CO) was re-examined for its anisotropy. The revised values are given here.

ponents are labeled assuming the positive sign for the hyperfine-coupling interaction.

The spectral pattern of the B signals seen in Figure 1 differs from that normally expected from an axially symmetric system on two accounts: (1) there are two signals labeled Q located midway between the outer pairs of the hyperfine components, and (2) the parallel signals of the first ($m_I = +^3/_2$) and the third ($m_I = -^1/_2$) hyperfine components are unusually strong in comparison with the associated perpendicular signals. Both features can be accounted for by the Au nuclear quadrupole interaction: the former by the forbidden transitions induced by the quadrupole term, and the latter by deprivation of the transition probability of the normal hyperfine components by the forbidden transitions in the perpendicular region.[11]

The spin Hamiltonian appropriate for Au(CO) is thus given as follows:

$$\hat{H}_{spin} = g_\parallel\beta H_z S_z + g_\perp\beta(H_x S_x + H_y S_y) + A_\parallel I_z S_z + A_\perp(I_x S_x + I_y S_y) + P_\parallel[I_z^2 - (1/3)I(I+1)] \quad (1)$$

Here the term involving $P_\parallel$ represents the nuclear quadrupole interaction and $P_\parallel$ is related to the nuclear quadrupole moment Q and the electric field gradient q as follows:

$$P_\parallel = \frac{3eqQ}{4I(2I-1)} = \frac{3eQ}{4I(2I-1)}\frac{\partial^2 V}{\partial z^2} \quad (2)$$

A treatment of eq 1 by the second-order perturbation theory has been shown by Bleaney.[12] A similar second-order treatment of a Hamiltonian for a more general orthorhombic case and a powder pattern spectrum simulation program based on its results have been described more recently.[13]

A preliminary analysis of the Au(CO) spectrum revealed that the resonance positions of the normal hyperfine components can be given with reasonable accuracy (within 10 G) by the second-order solution of eq 1 without the quadrupole term. We therefore simulated the spectrum using the **g** tensor ($g_\parallel = 1.975$, $g_\perp = 1.911$) and the ^{197}Au hyperfine-coupling tensor ($A_\parallel = 634$ G, $A_\perp = 639$ G) thus tentatively assessed and the quadrupole coupling constant ($P_\parallel$) varied successively for the best fit. Figure 3 shows the representative results. We thus concluded that $P_\parallel = 45$ (5) G.

Inspection of the second-order solution of eq 1 (including the quadrupole term)[11-13] reveals that, while the positions of the parallel signals of the normal hyperfine components are not affected by the quadrupole term, the perpendicular signals of the lower field hf components ($m_I = +^3/_2$ and $+^1/_2$) are shifted downfield by $3P_\parallel^2/(2A)$, while those of the higher field hyperfine components ($m_I = -^1/_2$ and $-^3/_2$) are shifted upfield by the same amount. For A and $P_\parallel$ assessed above, $3P_\parallel^2/(2A) = 5$ G. The resonance positions of "Au(CO) without the quadrupole term" could thus be determined accurately.

It has been shown that, for an axially symmetric system without the quadrupole term, the resonance fields $H_\parallel(m)$ and $H_\perp(m)$ are given exactly by the following "continued fraction" expressions.[14]

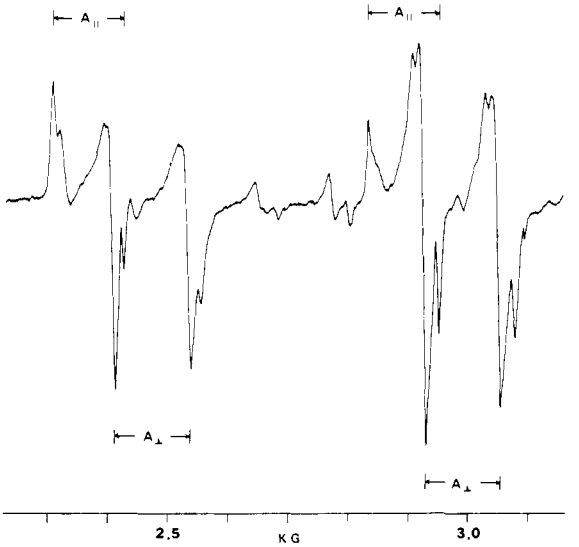

Figure 4. The lower field components ($m_I = +3/2$ and $+1/2$) of the B signals observed from the Au/^{13}CO(2%)/Ar system. The splittings due to $A_\parallel(^{13}C)$ and $A_\perp(^{13}C)$ are indicated.

$$H_\parallel(m) = H_\parallel^0 - mA_\parallel' - F_\parallel - G_\parallel$$

$$H_\perp(m) = H_\perp^0 - mA_\perp' - F_\perp - G_\perp \quad (3)$$

Here m indicates the hyperfine component ($m_I = m$),

$$F_\parallel = \frac{\eta_\parallel^2[I(I+1) - m(m+1)]}{H_\parallel(m) + (m+1/2)A_\parallel' + F_\parallel}$$

$$G_\parallel = \frac{\eta_\parallel^2[I(I+1) - m(m-1)]}{H_\parallel(m) + (m-1/2)A_\parallel' + G_\parallel}$$

$$F_\perp = \frac{\eta_\perp^2[I(I+1) - m(m+1)]}{H_\perp(m) + (m+1/2)A_\perp' + F_\perp}$$

$$G_\perp = \frac{\eta_\perp^2[I(I+1) - m(m-1)]}{H_\perp(m) + (m-1/2)A_\perp' + G_\perp}$$

$$H_\parallel^0 = h\nu/(g_\parallel\beta) \qquad H_\perp^0 = h\nu/(g_\perp\beta)$$

$$A_\parallel' = A_\parallel/(g_\parallel\beta) \qquad A_\perp' = A_\perp/(g_\perp\beta)$$

$$\eta_\parallel = A_\perp' g_\perp/(2g_\parallel) \qquad \eta_\perp = (A_\parallel' g_\parallel + A_\perp' g_\perp)/(4g_\perp)$$

From the resonance positions of the $m_I = \pm^3/_2$ components of "AuCO without the quadrupole term" and the equations given above for $H_\parallel(m)$ and $H_\perp(m)$, the consistent set of **g** and hyperfine-coupling tensors were determined by a computer-assisted iteration process. The results were as follows:

$$g_\parallel = 1.9791\ (6) \qquad g_\perp = 1.9105\ (6)$$

$$A_\parallel = 628.9\ (5)\ \text{G} \qquad A_\perp = 630.4\ (5)\ \text{G}$$

The resonance positions computed from eq 3 using these parameters (with corrections for the quadrupole term for the perpen-

(11) See, for example: Abragam, A.; Bleaney, B. "Electron Paramagnetic Resonance of Transition Ions"; Oxford: London, 1970; pp 178–186.
(12) Bleaney, B. *Philos. Mag.* **1951**, *42*, 441. See also, ref 11.
(13) Kasai, P. H.; McLeod, D., Jr.; Watanabe, T. *J. Am. Chem. Soc.* **1980**, *102*, 179.
(14) Kasai, P. H.; McLeod, D., Jr. *Faraday Discuss. Symp. 14, Chem. Soc.* **1980**, 65.

Table III. Analyses of the Hyperfine Coupling Tensors of Cu(CO), Ag(CO), and Au(CO) (A_{iso} and A_{dip} given in MHz)[a]

	metal hyperfine tensor				^{13}C hyperfine tensor			
carbonyl	A_{iso}	$\rho(ns)$	A_{dip}	$\rho(np)$	A_{iso}	$\rho(2s)$	A_{dip}	$\rho(2p)$
Cu(CO)	4142	0.67	16	0.16	180	0.05	−4	−0.04
Ag(CO)	1787	0.99	−5		38	0.01	2	0.02
Au(CO)	1705	0.54	19	0.55	327	0.09	−5	−0.05

[a] See text for the definitions of A_{iso} and A_{dip}, and the atomic values assumed in computing the unpaired electron density.

dicular signals) are compared with the observed values in Table I.

Figure 4 shows the lower field hyperfine components ($m_I = +^3/_2$ and $+^1/_2$) of Au(CO) observed from the Au/^{13}CO(2%)/Ar system. The doublet splittings due to a hyperfine interaction with one ^{13}C nucleus are clearly revealed as indicated. Similar splittings were observed for the higher field hyperfine components also. The ^{13}C hyperfine coupling tensor of Au(CO) was thus determined as follows:

$$|A_{\parallel}(^{13}C)| = 114\ (2)\ G \qquad |A_{\perp}(^{13}C)| = 124\ (2)\ G$$

Observation of the hyperfine interaction with one ^{13}C nucleus is a strong substantiation of the assignment of the B signals to Au(CO).

Discussion

Table II shows the **g** tensors and the hyperfine-coupling tensors of the metal and ^{13}C nuclei of Cu(CO) and Ag(CO) reported earlier[5,6] and those of Au(CO) determined presently. The hyperfine tensor elements determined in gauss were converted to those in MHz by multiplication by $g\beta$.

The large, essentially isotropic ^{197}Au hyperfine-coupling tensor of Au(CO) signifies a large unpaired electron density in the Au 6s orbital. The bonding scheme of Au(CO) must hence be similar to that of Cu(CO); the complex is held by the dative interaction between the lone-pair electrons of CO and the vacant sp_σ hybrid orbital of Au and the back-donation from the filled d_π orbitals of Au into the vacant π^* orbitals of CO. The unpaired electron is in the sp_σ hybrid orbital of Au pointing away from the ligand.

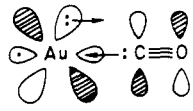

It has been shown that the principal elements, $A_\parallel$ and $A_\perp$, of an axially symmetric hyperfine tensor are related to the isotropic term, A_{iso}, and the orientation dependent part, A_{dip}, as follows.[15]

$$A_\parallel = A_{iso} + 2A_{dip}$$

$$A_\perp = A_{iso} - Ad_{ip} \qquad (4)$$

where

$$A_{iso} = g_e\beta_e g_n\beta_n(8\pi/3)|\phi(0)|^2$$

$$A_{dip} = g_e\beta_e g_n\beta_n\left\langle\frac{3\cos^2\alpha - 1}{2r^3}\right\rangle = g_e\beta_e g_n\beta_n\frac{2}{5}\left\langle\frac{1}{r^3}\right\rangle_p$$

Here $|\phi(0)|^2$ represents that spin density at the magnetic nucleus, r the separation between the nucleus and the electron, and α the angle between r and the symmetry axis. In an LCAO description of the semifilled orbital, only the spin density in an s orbital contributes to A_{iso} and that in a non s orbital to A_{dip}. The second expression for A_{dip} is for a unit spin density in a p_σ orbital.

Table III shows the A_{iso}'s and A_{dip}'s of the three carbonyls determined from the observed hyperfine tensors (Table II) and eq 4. Comparison of these values against the "atomic values" yields the spin densities in the respective valence orbitals as shown. For the atomic values $A_{iso}^0(M)$ the hyperfine-coupling constants determined earlier for the isolated atoms were chosen;[8] thus $A_{iso}^0(M)$ = 6151, 1810, and 3138 MHz for ^{63}Cu, ^{107}Ag, and ^{197}Au, respectively. The atomic values $A_{dip}^0(M)$ were estimated from the measured hyperfine-splitting terms a ($j = {}^1/_2$) of ^{69}Ga, ^{115}In, and ^{205}Tl atoms (ns^2np^1);[16] thus $A_{dip}^0(M)$ = 102, 29, and 34 MHz for ^{63}Cu, ^{107}Ag, and ^{197}Au. For the ^{13}C nucleus theoretically computed values, $A_{iso}^0(^{13}C)$ = 3780 and $A_{dip}^0(^{13}C)$ = 107 MHz, were used.[17]

The unpaired electron densities determined for the metal ns orbitals in Table III clearly predicate that while Cu(CO) and Au(CO) are bona fide complexes Ag(CO) is not. The latter has been concluded to be an Ag atom perturbed by the presence of CO in the nearest neighbor sphere of the host lattice.[6] The weak Ag–CO interaction in "Ag(CO)" is also evidenced in the negligible density in the Ag 5p orbital and in its anomalously small ^{13}C hyperfine-coupling tensor. The negative $A_{dip}(M)$ obtained for Ag(CO) has been attributed to admixture of the Ag4d_σ orbital in its semifilled orbital.[6]

It has been shown that, for a radical with a nondegenerate ground state $|0\rangle$, deviation of the g term from the spin only value g_e (=2.0023) is given by eq 5.[18] Here i (= x, y, z) represents a principal axis of the

$$g_i - g_e = -2\lambda\sum_n\frac{\langle 0|L_i|n\rangle\langle n|L_i|0\rangle}{E_n - E_0} \qquad (5)$$

g tensor, L_i the orbital angular momentum operator, and λ the one-electron spin–orbit coupling constant. The summation is performed for all the excited states. In evaluating eq 5 in terms of LCAO–MO's, only one-centered integrals may be retained, and for each atomic integral the spin–orbit coupling constant of the particular atom is used. Thus in the present situation where the semifilled orbital is given by $\Phi = \phi_M(ns) - b\phi_M((np_\sigma)$, only the $\phi_M(np_\sigma)$ part contributes to the deviation, and the excited states of importance are only those involving the vacant np_π orbitals of the metal atom. It thus follows that $g_\parallel - g_e = 0.0$ and $g_\perp - g_e < 0$. Indeed, for both Cu(CO) and Au(CO), the smallest deviation from the spin only value is seen in the parallel direction and a large negative shift in the perpendicular direction. The spin–orbit coupling constants of the Cu, Ag, and Au atoms in the $(n-1)d^{10}np^1$ state are 165, 613, and 2543 cm^{-1}, respectively.[19] A much larger shift observed for the $g_\perp$ of Au(CO) is thus accounted for. The g shift for Ag(CO) is essentially nill consistent with the orbital picture revealed from the Ag hyperfine-coupling tensor. That its $g_\perp$ is larger than $g_\parallel$ can be accounted for by admixture of 4d_σ orbital also indicated in the analysis of the Ag hyperfine-coupling tensor.

Figure 5 shows schematically the energy levels of the valence $(n-1)$d, ns, and np orbitals of the Cu, Ag, and Au atoms,[19] and those of the lone-pair electrons of CO and its vacant π^* orbitals.[20] For the Cu–CO pair, the metal d_π and CO π^* levels are close, but the metal s and CO lone-pair levels are far apart. We surmise that the $d_\pi \rightarrow \pi^*$ back-donation is primarily responsible for the formation of Cu(CO). The valence s and p orbitals of Ag are at essentially identical levels as those of Cu, but its 4d level is significantly lower than the Cu 3d level. Failure to form a bona

(15) Smith, W. V.; Sorokin, P. P.; Gelles, I. L.; Lasher, G. J. *Phys. Rev.* **1959**, *115*, 1546.

(16) Kopferman, H. "Nuclear Moments"; Academic Press: New York, 1958; pp 123–138. See also: Lindsay, D. M.; Kasai, P. H. *J. Magn. Reson.*, in press.

(17) Morton, J. R.; Preson, K. F. *J. Magn. Reson.* **1978**, *30*, 577.

(18) Pryce, M. H. L. *Proc. Phys. Soc., London, Sect. A.* **1950**, *63*, 25.

(19) Moore, C. E. *Natl. Bur. Stand. Circ. (U.S.) No. 467* **1949**, 1; **1952**, 2; **1958**, 3.

(20) Herzberg, G. "Molecular Spectra and Molecular Structure I. Spectra of Diatomic Molecules"; Van Nostrand Reinhold: New York, 1950.

fide Ag(CO) complex is attributed to an increased separation between the metal d_π and CO π^* levels. It is intruiguing that, for the Au–CO pair, the metal d_π and CO π^* levles are further apart than they are in the Cu–CO case, but the metal s and the CO lone-pair levels are closer. It is surmised that both the σ-type dative interaction by the CO lone-pair electrons and the $d_\pi \rightarrow \pi^*$ back-donation are operative in Au(CO). Ozin et al. reported the CO stretching frequencies of Cu(CO) and Au(CO) at 2010 and 2039 cm^{-1}, respectively,[2,4] indicating less back-donation for the latter. A larger σ-type dative interaction in Au(CO) is evidenced in its semifilled orbital showing a greater extent of sp_σ hybridization (Table III).

For an electron in a p orbital, the electric field gradient q in eq 2 is given by $e(4/5)\langle 1/r^3\rangle_p$. Hence if we assume that the electric field gradient at the Au nucleus in Au(CO) is generated mostly by the unpaired electron in the 6p orbital, the observed quadrupole coupling constant $P_\parallel$ is related to $\rho(6p)$ as follows:

$$P_\parallel = \rho(6p)\, P_\parallel{}^0 \qquad (6)$$

where

$$P_\parallel{}^0 = \frac{3e^2Q}{4I(2I-1)}\,\frac{4}{5}\left\langle\frac{1}{r^3}\right\rangle_p$$

Substitution of the known quadrupole moment of the ^{197}Au nucleus (0.59×10^{-24} cm^2) and 63×10^{24} cm^{-3} for $\langle 1/r^3\rangle$, a value estimated from the known hyperfine splitting term a ($j = {}^1/_2$) of ^{205}Tl atom ($6s^26p^1$),[16] yields $P_\parallel{}^0 = 259$ MHz. Thus the measured $P_\parallel$ gives $\rho(6p)$ of $\sim$0.50 in close agreement with the result obtained from the analysis of the Au hyperfine tensor.

In Table III the ^{13}C hyperfine tensors were analyzed assuming that $A_\parallel(^{13}C)$ and $A_\perp(^{13}C)$ were both positive. The A_{dip} defined in eq 4 is a positive quantity for an electron in a p_σ orbital. It follows that $A_\parallel > A_\perp$. Only the ^{13}C hyperfine tensor of Ag(CO) "pseudocomplex" conforms to this rule. The ^{13}C hyperfine tensor of Cu(CO) was earlier reported as being isotropic,[5] but a closer re-examination of the spectrum revealed that $|A_\parallel| < |A_\perp|$ as shown. The "$A_\parallel > A_\perp$" rule would be upheld for Cu(CO) and Au(CO) also, if we assume either that $A_\parallel > 0$ and $A_\perp < 0$ or that $A_\parallel < 0$ and $A_\perp < 0$. The former was ruled out since it gave an unreasonably large unpaired electron density ($\rho > 1.0$) in the C $2p_\sigma$ orbital. The latter was also deemed unlikely since it yielded an unusually large negative density in the C 2s orbital. The negative A_{dip}'s concluded for the ^{13}C hyperfine tensors of Cu(CO) and Au(CO) can be accounted for, for example, by some unpaired electron density in the C $2p_\pi$ orbitals. The analyses of the **g** tensors have already shown admixture of the π MO's (consisting primarily of the metal np_π and C $2p_\pi$ orbitals) into the semifilled orbitals of Cu(CO) and Au(CO). It is apparent that the ^{13}C hyperfine tensors of Cu(CO) and Au(CO) are fundamentally different from that of Ag(CO).

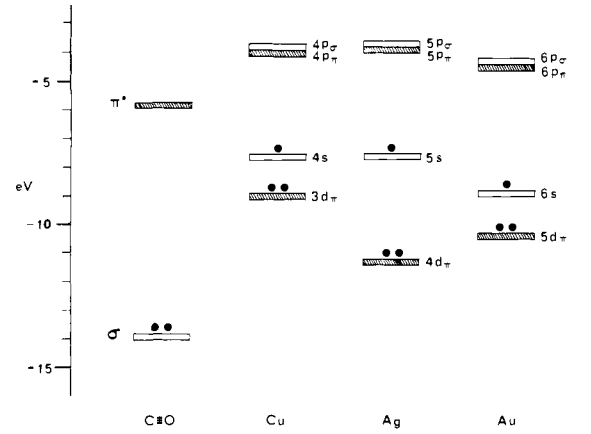

Figure 5. The energy levels of the valence $(n-1)$d, ns, and np orbitals of the Cu, Ag, and Au atoms and those of the lone-pair electrons of CO and its vacant π^* orbitals.

The inability of the Au atom to form $Au(CO)_3$ while it could form both the bona fide mono- and dicarbonyl complexes eludes a simple explanation. We may note that the back-donation occurs only from the metal d_π orbitals in the monocarbonyls presently being discussed, from both the d_π orbitals and the semifilled metal p_π orbital in the dicarbonyls of a linear structure, and only from the semifilled metal p_π orbital in the trigonal-planar tricarbonyls. The failure to form $Au(CO)_3$ may thus, in part, be attributed to a higher (by $\sim$1 eV) $ns \rightarrow np$ promotion energy of the Au atom.

Registry No. Au(CO), 60594-88-9.